Title
Tyrosinase-Mediated Synthesis of Nanobody—Cell Conjugates

Journal
ACS Central Science, 8(7)

ISSN
2374-7943

Authors
Maza, Johnathan C
García-Almedina, Derek M
Boike, Lydia E
et al.

Publication Date
2022-07-27

DOI
10.1021/acscentsci.1c01265

ACS central science

http://pubs.acs.org/journal/acscii

Research Article

Tyrosinase-Mediated Synthesis of Nanobody–Cell Conjugates

Johnathan C. Maza, Derek M. García-Almedina, Lydia E. Boike, Noah X. Hamlish, Daniel K. Nomura, and Matthew B. Francis*

Cite This: *ACS Cent. Sci.* 2022, 8, 955–962

Read Online

ACCESS | Metrics & More | Article Recommendations | Supporting Information

ABSTRACT: A convenient enzymatic strategy is reported for the modification of cell surfaces. Using a tyrosinase enzyme isolated from *Agaricus bisporus*, unique tyrosine residues introduced at the C-termini of nanobodies can be site-selectively oxidized to reactive *o*-quinones. These reactive intermediates undergo rapid modification with nucleophilic thiol, amine, and imidazole residues present on cell surfaces, producing novel nanobody–cell conjugates that display targeted antigen binding. We extend this approach toward the synthesis of nanobody–NK cell conjugates for targeted immunotherapy applications. The resulting NK cell conjugates exhibit targeted cell binding and elicit targeted cell death.

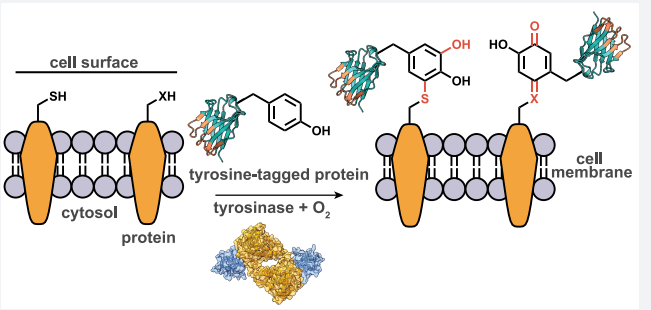

INTRODUCTION

Cells are the basic units of life and are capable of dynamically sensing and responding to their environments through biomolecular interactions on their surfaces. As such, the ability to manipulate the cell surface has a broad range of applications in basic and applied science. For example, the attachment of DNA oligonucleotides to cells has enabled their controlled adhesion to glass surfaces and gold electrodes,[1−3] and the decoration of different cells with complementary DNA strands has allowed the formation of controlled cell–cell contacts.[4] Finally, the introduction of cancer-antigen-binding paratopes to the surfaces of immune cells has led to the development of cell-based immunotherapies against a variety of cancers.[5] While genetic engineering has been a key technology in many of these applications, new chemistries are emerging for the direct attachment of complex molecules to cell surfaces.[6] These methods could help overcome challenges associated with viral transduction vectors, like batch-to-batch heterogeneity and long-term safety concerns, while also representing a means for the scalable preparation of novel cell conjugates.[7−9]

Chemistries that modify cells must perform under a narrow set of conditions in order to maintain cell viability. They must proceed in buffered aqueous media at the optimal physiological pH—typically pH 7.4—and within a temperature range of 4–37 °C. Furthermore, these reactions must have sufficiently rapid kinetics to achieve high conversion even when confronted with the limits of surface diffusion characteristics. Due to these requirements, few chemistries exist that can attach molecules and proteins to live cells. A notable example includes metabolic engineering using unnatural oligosaccharides. This enables the decoration of cell surfaces with biorthogonal azide handles for subsequent modification with phosphine- or cyclooctyne-containing cargo.[10−12] This approach has also been used to engineer new interactions between immune cells and cancer.[13] Installation of DNA molecules onto cell surfaces has enabled the hybridization-directed installation of full-length IgG onto cell surfaces with applications in immunotherapy.[14,15] Finally, enzymes like sortase,[16,17] asparaginyl ligase,[18] and fucosyltransferase[19] have all been used to catalyze the attachment of small molecules and proteins to cells.

Recently, the enzyme tyrosinase has emerged as a useful tool for site-selective protein modification.[20−23] Canonically, the enzyme acts on free tyrosine amino acids to catalyze their oxidation to highly reactive *o*-quinone intermediates in the biosynthesis of melanin. Over the last two decades, our lab has used these *o*-quinones to modify protein N-termini (especially proline N-termini) as well as free thiols present on proteins (Figure 1a).[20,21] Recent advances have shown that the tyrosinase from *Agaricus bisporus* (abTYR) is also capable of oxidizing engineered tyrosine tags, like Ser–Gly_4–Tyr tags at protein C-termini. This produces *o*-quinones in specific locations on protein surfaces, which can then be intercepted by a variety of small-molecule- or protein-based nucleophiles.[21−23] This strategy has been shown previously for the site-specific modification of both tyrosine-tagged single-chain variable fragments and full-length IgG.[21−23]

Herein, we adapt and expand this bioconjugation chemistry to achieve the one-step attachment of tyrosine-tagged proteins

Received: October 13, 2021
Published: June 22, 2022

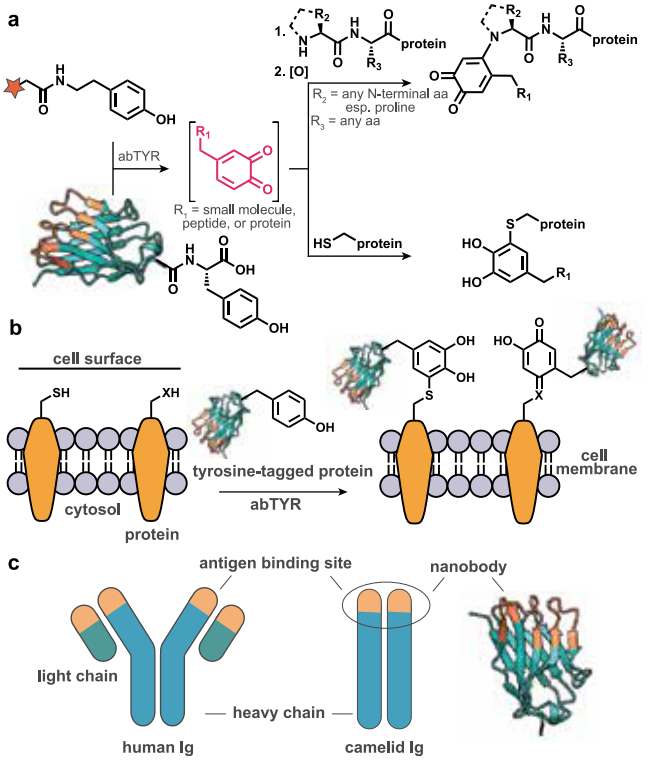

Figure 1. General strategy for modifying cell surfaces with nanobodies. (a) Tyrosinase catalyzes the oxidation of small-molecule phenols to highly reactive *o*-quinones, which can modify nucleophiles present on proteins. Engineered tyrosine tags at protein termini can also be oxidized by tyrosinase, producing a site-specific *o*-quinone on the protein that reacts with protein-based nucleophiles. (b) Tyrosine-tagged nanobodies can be site-specifically oxidized by tyrosinase for attachment of these proteins to cells. The resulting linkage produces a well-defined point of attachment for installing nanobodies on cell surfaces while imbuing the target cell with novel antigen-binding functionality. (c) Nanobodies are low-molecular-weight (~10−15 kDa) antigen-binders derived from the variable region of the camelid antibody (PDB ID 3K1K).

to cell surfaces. In this approach, a protein of interest is expressed with a C-terminal tyrosine, such as the sequence described above. The protein can be mixed with cells of interest and abTYR for site-selective activation of the introduced tyrosine to the corresponding *o*-quinone intermediate. These C-terminal *o*-quinones then react with endogenous nucleophiles present on cell surfaces, producing well-defined points of attachment (Figure 1b).

To demonstrate the applicability of this approach, we generated tyrosine-tagged nanobodies, which are small antigen-binders derived from the variable regions of camelid immunoglobulins (Figure 1c).[24] We show that abTYR site-specifically oxidizes introduced tyrosine tags and mediates the attachment of nanobodies to cell surfaces while retaining their antigen-binding abilities. We extend this strategy toward the synthesis of nanobody−natural killer (NK) cell conjugates, which exhibited targeted cell lysis. This strategy thus provides a simple, direct synthetic alternative to genetic engineering for cell-based immunotherapy applications.

RESULTS AND DISCUSSION

Tyrosinase-Mediated Synthesis of Nanobody−Cell Conjugates. To begin, a previously reported nanobody against GFP was expressed with a C-terminal Ser−Gly_4−Tyr tag ($nbGFP_{Tyr}$).[25] To test the ability of abTYR to selectively oxidize the introduced tyrosine tag, 10 μM $nbGFP_{Tyr}$ was exposed to 400 nM abTYR at 37 °C. A time-course experiment was performed, and analysis using ESI-TOF mass spectrometry revealed that the $nbGFP_{Tyr}$ was fully converted to a singly oxidized product after 10 min, as indicated by a mass shift of ~14 Da (Figure 2a and Supplementary Figure S1). Importantly, if the tyrosine residue in the tyrosine tag was swapped for a cysteine ($nbGFP_{Cys}$) no change in molecular weight was observed in the ESI-TOF MS trace, and no disulfide was formed. Taken together, these results indicate that it is the single phenol in the C-terminal tyrosine tag being oxidized by abTYR, providing a uniquely reactive *o*-quinone on

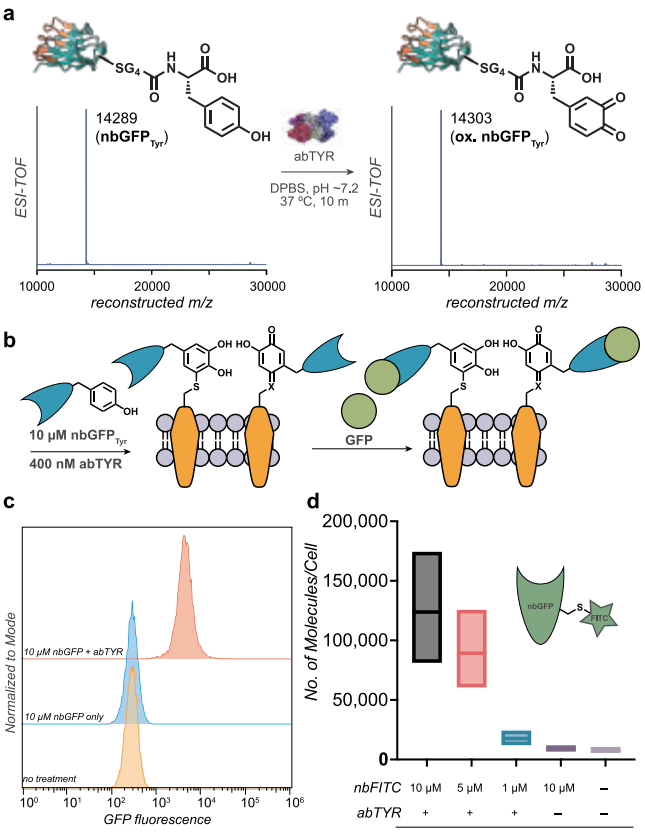

Figure 2. Modification of NK cell surfaces with nanobodies. (a) Tyrosinase enzyme produces a site-specific *o*-quinone at the C-terminal Ser−Gly_4−Tyr tag installed on nanobodies, as evidenced by a 14 Da mass shift detected via ESI-TOF MS. (b) To verify that NK cell surfaces can be decorated with nanobodies using tyorsinase, a Tyr-tagged nanobody against GFP ($nbGFP_{Tyr}$) was designed. Using tyrosinase, $nbGFP_{Tyr}$ can be attached to the cell surface, and 2° labeling with GFP can be used to analyze the reaction using flow cytometry. (c) Labeling experiments with $nbGFP_{Tyr}$ validated attachment of the nanobody to the cell surface, as only cells treated with both $nbGFP_{Tyr}$ and tyrosinase showed an increase in GFP fluorescence (red trace) over controls (blue and orange traces). (d) Using a Cys point mutant, a single FITC dye can be attached to each $nbGFP_{Tyr}$ (nbFITC). After attachment of 10 μM nbFITC to cell surfaces, comparison against FITC-calibration beads determined that a median value of ~120,000 copies of the nanobody were linked to the cells. Data are represented as box plots, with the top of the box representing the 75th percentile of the data, the middle line representing the median of the data, and the bottom of the box representing the 25th percentile of the data.

https://doi.org/10.1021/acscentsci.1c01265
ACS Cent. Sci. 2022, 8, 955−962

the nanobody for attachment to cell surfaces (Supplementary Figure S1). This is in good agreement with previous work demonstrating the site-specific oxidation of tyrosine-tagged proteins.[21−23]

Next we explored the ability of abTYR to catalyze the attachment of nbGFP$_{Tyr}$ to cell surfaces. As a model cell system, we used NK cells, which have recently emerged as promising agents for targeted immunotherapies. Like T-cells, NK cells possess cytotoxic effector functions, and studies have shown that adoptively transferred NK cells are less prone to host rejection than their T-cell counterparts.[26,27] Additionally, methods for generating a robust supply of immortalized NK cells have been developed, enabling the scalable synthesis of engineered NK variants. NK-92MI is an immortalized NK cell line that constitutively expresses the gene for hIL-2, a cytokine required for NK cell proliferation and activation, facilitating cell culture and analysis of downstream effector functions.[28,29] However, these cells do not express Fc receptors, limiting their use in antibody-dependent cell cytotoxicity applications. Thus, the direct modification of this cell type with novel antigen-binding functionalities would provide exciting avenues for the synthesis of "off-the-shelf" NK-based immunotherapeutics.

As an initial proof of concept, ∼1 × 10^6 NK-92MI cells were exposed to 10 μM nbGFP$_{Tyr}$ with 400 nM abTYR for 10 min at 37 °C in a cell incubator under 5% CO_2. To validate successful attachment of the nbGFP$_{Tyr}$ to the cell surfaces, cells were washed and subjected to a secondary labeling step with 1 μM sfGFP for 30 min (Figure 2b). After any unbound sfGFP was washed away, cells were analyzed for GFP fluorescence using flow cytometry. An increase in GFP fluorescence was only detected in the cells that had been treated with both nbGFP$_{Tyr}$ and abTYR (Figure 2c, red trace). Cells exposed to only nbGFP$_{Tyr}$ showed no change in fluorescence over no treatment controls (Figure 2c, blue and orange traces). These results indicate that the oxidation of nbGFP$_{Tyr}$ by abTYR facilitates covalent attachment of the nanobody to the cell surface and that the attached nanobody retains antigen binding. Importantly, cell viability was unchanged after modification, as no increase in propidium iodide signal, a fluorescent indicator of cell death, was detected for those NK cells modified with nanobodies over controls (Supplementary Figure S2). In addition, half-life studies were also performed. It was determined that the attached nanobodies were retained on the cell surfaces with a half-life of ∼7.8 h (Supplementary Figure S3). This is comparable to other techniques that covalently attach proteins to the cell surface[14,19] and means NK cell surfaces should be returned to their unmodified state within 48 h.

To determine the number of nanobodies that were attached to the cell surface, we generated an nbGFP$_{Tyr}$ bearing an alanine to cysteine mutation at position 76. We then site-specifically attached a maleimide−FITC dye to this cysteine (nbFITC, Supplementary Figure S4). Treatment of cells with this construct and abTYR resulted in attachment of nbFITC to the cell surface. Since a single FITC molecule is on every nanobody, comparison of the nbFITC-labeled cells to FITC calibrant beads, which contain a known number of FITC molecules, enabled the determination of the number of nanobodies on each cell surface. Using this approach, it was determined that a median of ∼120,000 copies of the nanobody were attached to each NK-92MI cell surface upon exposure to 10 μM nanobody and 400 nM abTYR for 10 min. The amount of nbFITC deposited on the cell surface can be tuned, as lower concentrations of the nanobody resulted in less modification. However, even nanobody concentrations as low as 1 μM resulted in fluorescence labeling above background levels (Figure 2d).

As a comparison, we also performed labeling reactions on Jurkat cells, an immortalized T-cell line. Approximately ∼1 × 10^6 Jurkat cells were incubated with varying concentrations of nbFITC in the presence or absence of 400 nM abTYR. After incubation for 10 min at 37 °C, cells were washed and analyzed for FITC fluorescence using flow cytometry. Jurkat cells exposed to both nbFITC and abTYR showed an increase in FITC signal over nbFITC only and untreated controls (Supplementary Figure S5). Once again, cell viability remained unchanged after modification, as no increase in propidium iodide signal was observed (Supplementary Figure S5). Comparison against FITC-calibration beads showed that using 10 μM nbFITC and 400 nM abTYR attached a median of ∼210,000 copies of the nanobodies to the cell surface (Supplementary Figure S5). Nanobody attachment could be tuned, with concentrations of nanobody as low as 1 μM resulting in fluorescence labeling over controls.

We also modified human PBMCs using this same approach. Gratifyingly, we see similar increases in fluorescence only when PBMCs are exposed to both 10 μM nbGFP$_{Tyr}$ and 400 nM abTYR while retaining high cell viability (Supplementary Figure S6).

To validate that nanobody attachment was occurring at the cell surface, Jurkat cells were modified with 10 μM nbFITC in the presence or absence of 400 nM abTYR. After reaction, the cell membrane was then labeled with a cell-membrane-specific far-red dye. Imaging using a confocal microscope revealed distinct halos of FITC signal only in the cells treated with nbFITC and abTYR, which colocalized with the cell membrane dye (Supplementary Figure S7). Some nonspecific binding of nbFITC was observed in cells treated with nbFITC in the absence of abTYR, but no clear halo was observed.

Jurkat cells are a robust cell line and can be easily cultured to produce large quantities of cells. As a result, they are a useful cell line for proteomics experiments, which often require large amounts of cellular material. To understand the nature of the site of attachment between the cell surface and tyrosine-tagged nanobodies, we designed a proteomics experiment using an alkynyl-tyramide handle. This small-molecule probe has a phenol moiety for abTYR activation and attachment to cellular proteins as well as a terminal-alkyne moiety for reaction with azide-bearing molecules in a Cu(II)-mediated azido-alkyne cycloaddition. To ∼100 × 10^6 Jurkat cells was added 100 μM alkynyl-tyramide probe and 400 nM abTYR to a final volume of 10 mL. Cells were incubated at 37 °C for 20 min and then washed. After washing, cells were lysed, and modified proteins were labeled with an N_3-TEV-biotin peptide tag. Proteins were then bound to a streptavidin−agarose resin and trypsin digested. Alkynyl-tyramide probe-modified peptides were released using TEV protease and then analyzed using mass spectrometry (Supplementary Figure S8).

Proteomic analysis identified 437 unique peptide sequences modified with the alkynyl-tyramide probe. Analysis of the amino acid residues modified with the probe identified lysine (50.6% of modified residues), histidine (30.2% of modified residues), and cysteine (19.2% of modified residues) as the nucleophilic sites responsible for modification (Supplementary Figure S8). While modification of thiol groups with abTYR-generated *o*-quinones has already been established, to the best

https://doi.org/10.1021/acscentsci.1c01265
ACS Cent. Sci. 2022, 8, 955−962

of our knowledge, this is one of the first examples of *o*-quinones reacting with the amines and imidazoles of lysine and histidine. In purified protein labeling reactions, off-target modification with lysine and histidine residues has not been observed, even when the protein being modified contains a highly solvent-accessible His_6 tag for purification. However, our previous work screening peptide N-termini for their ability to be modified by *o*-quinones found that both primary and secondary amines can be modified using this approach.[30] It is not unreasonable that reactions involving these residues are captured in our proteomics experiment. It is also possible that the modifications observed represent unique reactive contexts on the cell surface, where the heterogeneity of proteins, nucleophiles, and solvent-accessible sites combine to afford unanticipated modifications. While we are further exploring the nature of these reactions on cell surfaces, we stress that solution-based oxidative couplings using purified proteins proceed with excellent chemoselectivity.[20−22]

We also analyzed the uniquely identified proteins based on their annotated subcellular localization. We found that only ∼23% of the identified proteins represented known cell membrane or secreted proteins, with the rest of the annotations representing proteins inside the cell, suggesting that this small-molecule probe is capable of crossing the cell membrane before it quenches (Supplementary Figure S8). This is not surprising, as a paper published while this Article was under review also found that tyrosinase-generated small-molecule *o*-quinones can be used to label intracellular proteomes.[31]

To explore if our small-molecule proteomics data were representative of the modifications using tyrosine-tagged proteins, we performed a proteomics experiments using a biotinylated $nbGFP_{Tyr}$ as bait (nbBAIT). After labeling the cell surface with this nanobody, we lysed the cells and captured any protein modified by the biotinylated nbBAIT protein using a streptavidin−agarose resin. The proteins were digested using trypsin, and the resulting peptides were submitted for proteomic analysis. Of the proteins captured in this experiment, only nine overlapped with the small-molecule proteomics experiment. Seven of these proteins have a known extracellular annotation and represent unique peptides in our small-molecule experiment that showed cysteine, lysine, and histidine modifications (Supplementary Figure S9).

Targeted Cell−Cell Interactions in abTYR-Synthesized Nanobody−NK Cell Conjugates. Once conditions for the attachment of nanobodies to cell surfaces had been established, we next explored the ability of nanobody−cell conjugates to engage in targeted cell−cell interactions. For this, we expressed a previously reported nanobody that binds the human epidermal growth factor receptor 2 (HER2) with the same C-terminal Ser−Gly_4−Tyr tag ($nbHER2_{Tyr}$).[24,32] The upregulation of HER2 is a hallmark of many breast cancers and makes targeting this receptor relevant for therapeutic purposes. Many HER2 targeting drugs are already available in the clinic where they show great efficacy against HER2+ cancers.[33]

To validate that the conjugation of $nbHER2_{Tyr}$ to proteins on the cell surface would not perturb HER2 binding, we synthesized a $nbHER2_{Tyr}$−sfGFP conjugate using a sfGFP Y200C mutant and abTYR. When exposed to the HER2+ cell line SK-BR-3, this construct produced a distinct shift in fluorescence indicative of successful binding. In comparison, the HER2− cell line MDA-MB-468 exhibited no change in fluorescence, indicating that the *o*-quinoid linkage connecting the two proteins did not lead to off-target binding (Supplementary Figure S10).

Once again, 1×10^6 NK-92MI cells were treated with 10 μM $nbHER2_{Tyr}$ in the presence or absence of 400 nM abTYR for 10 min at 37 °C and with 5% CO_2. After washing, the cells were assayed for their ability to bind FITC-labeled HER2 in solution. Only cells treated with the combination of $nbHER2_{Tyr}$ and abTYR were able to bind FITC-labeled HER2, as evidenced by a shift in the population of cells exhibiting fluorescence over an untreated control (Figure 3a, red trace). No shift in fluorescence was observed for cells treated with $nbGFP_{Tyr}$ and abTYR (Figure 3a, blue trace). This indicates that antigen-binding of the conjugates is dependent on the target of the nanobody and is not influenced by the *o*-quionone-derived linkage between the nanobody and the cell surface.

An important component of NK engagement is the binding of these cells to cell targets. To validate that tyrosinase-synthesized NK−$nbHER2_{Tyr}$ could bind HER2+ cells, nanobody−NK conjugates were synthesized as described above. After synthesis, the conjugated NK cells were labeled with a MitoTracker Red dye. Simultaneously, the HER2+ cell line SK-BR-3 was labeled with a green CFSE dye, and the two cell types were mixed at a ratio of 2:1 (NK-conjugate:SK-BR-3). Cells were allowed to bind and settle for 2 h at 37 °C and 5% CO_2, after which they were imaged using a high-throughput fluorescence microscope (ImageXpress Micro, Molecular Devices). A nearest neighbor analysis was performed using CellProfiler (Broad Institute) to determine the number of red-labeled NK cells touching each green-labeled target SK-BR-3 cell. A greater proportion of green target cells were bound by two or more red NK cells only if they had been pretreated with 10 μM $nbHER2_{Tyr}$ and 400 nM abTYR for 10 min (Figure 3b, orange bar). Absence of abTYR or conjugation with $nbGFP_{Tyr}$ resulted in no statistically significant binding of target cells over untreated controls (Figure 3b, blue bars). Finally, a rosette pattern of binding between the green HER2+ cells and the red NK cells, commonly observed when cells are forming cell:cell contacts, was only observed for NK cells treated with $nbHER2_{Tyr}$ and abTYR (Figure 3c). Taken together, these results indicate that the tyrosinase-synthesized nanobody−NK conjugates form specific contacts with HER2+ cell types in a manner dependent on the antigen target of the nanobody.

Targeted Killing of $nbHER2_{Tyr}$−NK Cell Conjugates. Finally, we explored the ability of tyrosinase-synthesized nanobody−NK conjugates to perform their effector functions and elicit targeted cell death. We used a fluorescence-based assay to measure NK-induced cell lysis. Briefly, HER2+ SK-BR-3 cells were preloaded with calcein AM dye, which becomes cell-impermeable after uptake. NK-induced cell death permeabilizes the cell membrane, and leakage of the dye into the supernatant allows fluorescent determination of NK cytotoxicity (Figure 4a).

NK-92MI cells were treated with $nbHER2_{Tyr}$ in the presence or absence of abTYR. As an isotype control, NK cells were also treated with $nbGFP_{Tyr}$ and abTYR. After treatment, cells were mixed with the calcein AM-labeled SK-BR-3 cells at a ratio of 5:1 (NK:SK-BR-3) and allowed to interact at 37 °C and 5% CO_2. After 4 h, cells were spun down, and the supernatant was harvested for fluorescence determination. A statistically significant cytotoxic response was only observed in the NK cells pretreated with both $nbHER2_{Tyr}$ and abTYR (Figure 4a, orange bar). Exposure of NK cells to $nbHER2_{Tyr}$ alone did not

https://doi.org/10.1021/acscentsci.1c01265
ACS Cent. Sci. 2022, 8, 955−962

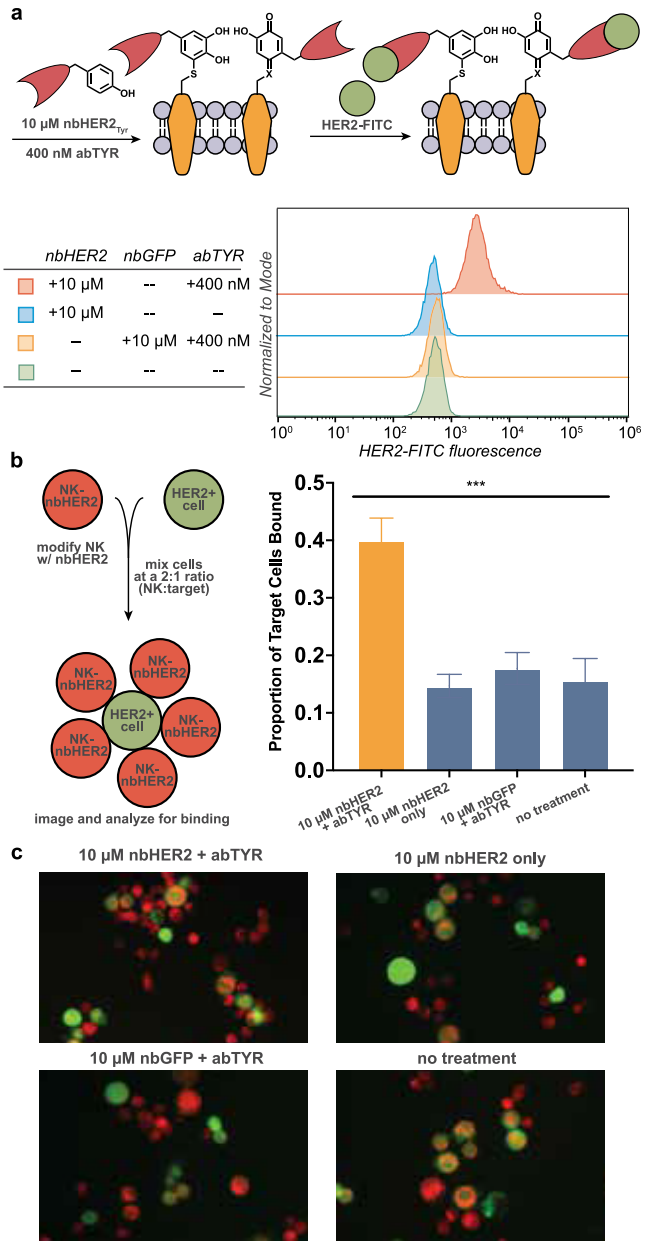

Figure 3. Decoration of NK cells for nanobody-directed cell−cell interactions. (a) Using tyrosinase, a Tyr-tagged nanobody against HER2 (nbHER2$_{Tyr}$) was attached to NK cells. Secondary labeling with a soluble FITC−HER2 showed that only cells exposed to nbHER2$_{Tyr}$ and tyrosinase exhibited a shift in FITC signal detected via flow cytometry (red trace) over controls. (b) To assess if tyrosinase-synthesized NK−nbHER2 conjugates can make targeted contacts with HER2+ cells, NK−nbHER2 cells were mixed with a HER2+ cell line (SK-BR-3) at a ratio of 2:1 (NK:target). Cells were allowed to bind and settle and then imaged using fluorscence microscopy. A nearest neighbor analysis was performed (CellProfiler), indicating that a statistically significant proportion of target cells (green) were bound to two or more NK−nbHER2 cells (red) only when the NK cells were pretreated with nbHER2$_{Tyr}$ and tyrosinase (orange bar). (c) Fluorescence microscopy images confirm rosette formation is only seen when NK cells are pretreated with both nbHER2$_{Tyr}$ and tyrosinase.

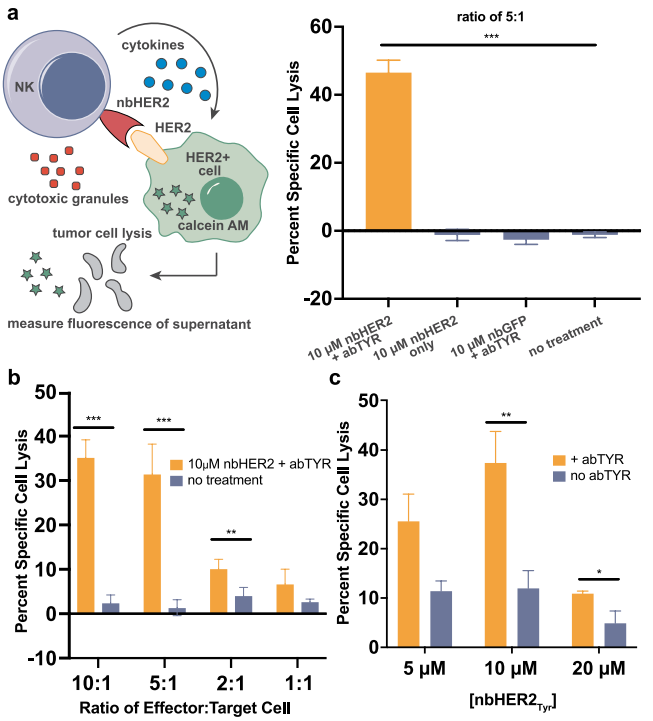

Figure 4. Targeted cell killing elicited by tyrosinase-synthesized nanobody−NK cell conjugates. (a) Schematic representation of the fluorescence-based cell assay used to determine NK cytotoxicity. HER2+ cells (SK-BR-3) were preloaded with calcein AM dye, which is retained by the cell membrane after uptake. Lysis of the HER2+ cell releases dye into the supernatant, providing a measurement for cell lysis. Only NK cells pretreated with both nbHER2$_{Tyr}$ and tyrosinase (orange bar) show statistically significant specific cell lysis over control treatments. (b) To assess how the ratio of NK:target cell impacts specific cytotoxicity, NK−nbHER2 cells were synthesized using 10 μM nbHER2$_{Tyr}$ and 400 nM tyrosinase and mixed with calcein AM loaded HER2+ cells (SK-BR-3). Statistically significant cell death was observed at ratios even as low as 2:1 (effector:target). (c) To assess the required concentration of nbHER2$_{Tyr}$ needed to elict NK-mediated cell death, a variety of concentrations of nbHER2$_{Tyr}$ were used to label NK cells with tyrosinase. Increased lysis was observed when using 5 and 10 μM nbHER2, while a sharp reduction of NK lytic activity was observed at the higher concentration of 20 μM nbHER2$_{Tyr}$.

elicit any significant response over no treatment controls, indicating that the cytotoxic response requires direct conjugation between the nanobody and the cell surface (Figure 4a). In addition, no significant cell death was observed in NK cells conjugated to nbGFP$_{Tyr}$ via abTYR (Figure 4a). This indicates that it is not the *o*-quinone-derived linkage between the nanobody and the cell surface nor the exposure of the NK cells to abTYR itself that results in cell lysis. Upon varying the ratio of NK−nbHER2$_{Tyr}$ conjugates to SK-BR-3 cells, we found that the conjugates were capable of eliciting targeted cell death even at ratios as low as 2:1 (NK-conjugate:SK-BR-3, Figure 4b).

We also examined how different concentrations of nbHER2$_{Tyr}$ in the abTYR coupling step affected the lysis ability of the resulting NK cell conjugates. An increase in the ability of the NK-conjugates to elicit cell death was observed when they were exposed to nbHER2$_{Tyr}$ concentrations up to 10 μM. At the highest nbHER$_{Tyr}$ concentration of 20 μM, however, the sharp decrease in cell lysis ability suggests that there is an optimal density of binding proteins on the cell surfaces, beyond which the NK cells lose their ability to engage their effector functions (Figure 4c). It is likely that very high

https://doi.org/10.1021/acscentsci.1c01265
ACS Cent. Sci. 2022, 8, 955−962

levels of nanobody labeling preclude the binding of NK activating receptors to their cognate ligands.

One mechanism by which NK cells mediate their cytotoxic functionality is through NKG2D engagement of MICA/B on target cell surfaces.[34] As such, we explored the role of the NKG2D-MICA/B axis in the cell death mediated by our synthesized NK−nbHER2$_{Tyr}$ conjugates. We performed the same cell killing assays as above but blocked either NKG2D on the NK cell or MICA/B on the SK-BR-3 target cell using their respective antibodies. As expected, when MICA/B was blocked on the target cell, a statistically significant reduction in cell death was observed when compared to an isotype control (Supplementary Figure S11). Interestingly, blocking NKG2D had no effect compared to an isotype control (Supplementary Figure S11). Modification of the NKG2D receptor by our conjugated nanobody may occlude the antibody epitope. However, the marked decrease in cell killing observed after blocking MICA/B indicates that the NKG2D receptor−ligand axis can still engage and plays an important role in mediating the cell killing we have observed.

CONCLUSION

Here, we have shown that the enzyme tyrosinase is capable of mediating the modification of nonengineered cell surfaces with full-size protein molecules. Using abTYR, unique tyrosine residues on the C-termini of nanobodies can be site-selectively oxidized. The resulting *o*-quinones undergo rapid reactions with amine- and thiol-based nucleophiles present on cell surfaces, as evidenced by proteomic analysis. Attachment of tyrosine-tagged proteins to the cell surface reached completion in ∼10 min and with no observed changes to cell viability. The resulting nanobody−cell conjugates are imbued with novel antigen-binding functionality, and we displayed the utility of this approach by synthesizing nbHER2-NK conjugates capable of eliciting targeted cell death in HER2+ model cell lines, with optimal cell killing occurring with the use of 10 μM of nbHER2$_{Tyr}$. It is likely that different nanobody modification levels will be optimal for different types of immune cells and applications. A clear benefit of this approach is the ability to tune the level of modification by controlling the amount of protein used in the tyrosinase coupling reaction. Given the ease with which tyrosine tags can be introduced at protein C-termini during recombinant expression, we anticipate this approach will facilitate the attachment of a variety of different protein substrates to cell surfaces, including other tyrosine-tagged nanobodies, single-chain variable fragments, and even full-length IgG. Finally, the reliance of the method on low enzyme concentrations facilitates subsequent processing steps and offers excellent potential for the scalable synthesis of protein−cell conjugates in the future.

ASSOCIATED CONTENT

Supporting Information

The Supporting Information is available free of charge at https://pubs.acs.org/doi/10.1021/acscentsci.1c01265.

Raw peptide lists for small-molecule proteomics (XLSX)

Unique peptides for small-molecule proteomics (XLSX)

Full experimental details and cloning procedures (PDF)

AUTHOR INFORMATION

Corresponding Author

Matthew B. Francis − *Department of Chemistry, University of California, Berkeley, California 94720, United States; Materials Sciences Division, Lawrence Berkeley National Laboratories, Berkeley, California 94720, United States;* orcid.org/0000-0003-2837-2538; Email: mbfrancis@berkeley.edu

Authors

Johnathan C. Maza − *Department of Chemistry, University of California, Berkeley, California 94720, United States;* orcid.org/0000-0003-2898-8770

Derek M. García-Almedina − *Department of Chemistry, University of California, Berkeley, California 94720, United States;* orcid.org/0000-0002-0679-6930

Lydia E. Boike − *Department of Chemistry, University of California, Berkeley, California 94720, United States; Novartis-Berkeley Center for Proteomics and Chemistry Technologies, Cambridge, Massachusetts 02139, United States*

Noah X. Hamlish − *Department of Molecular and Cell Biology, University of California, Berkeley, Berkeley, California 94720, United States*

Daniel K. Nomura − *Department of Chemistry, University of California, Berkeley, California 94720, United States; Novartis-Berkeley Center for Proteomics and Chemistry Technologies, Cambridge, Massachusetts 02139, United States; Department of Molecular and Cell Biology and Department of Nutritional Sciences and Toxicology, University of California, Berkeley, Berkeley, California 94720, United States; Innovative Genomics Institute, Berkeley, California 94720, United States;* orcid.org/0000-0003-1614-8360

Complete contact information is available at: https://pubs.acs.org/10.1021/acscentsci.1c01265

Author Contributions

The manuscript was written through contributions of all authors. All authors have given approval to the final version of the manuscript.

Notes

The authors declare no competing financial interest.

ACKNOWLEDGMENTS

This work was supported by the N.I.H. (R01GM138693) as well as the Chemical Biology Graduate Program at UC Berkeley (NIH T32-GM066698). J.C.M. was supported by a UC Berkeley Fellowship for Graduate Studies, and J.C.M. and L.B. were both supported by NSF Graduate Research Program Fellowships. D.M.G.A. was supported by a UC Berkeley Chancellor Fellowship. The authors thank Paul Huang for assistance in confocal imaging. The authors thank Dr. Mary West for flow cytometry and microscopy resources through the QB3 Cell and Tissue Analysis Facility.

ABBREVIATIONS

abTYR = tyrosinase from *Agaricus bisporus*
sfGFP = superfolder green fluorescent protein
nbGFP$_{Tyr}$ = GFP-binding nanobody with C-terminal Ser−Gly$_4$−Tyr tag

nbGFP$_{Cys}$ = GFP-binding nanobody with C-terminal Ser−Gly$_4$−Cys tag
nbFITC = A76C mutant of nbGFP$_{Tyr}$, modified with FITC-maleimide
HER2 = Human epidermal growth factor receptor 2
nbHER2$_{Tyr}$ = HER2-binding nanobody with C-terminal Ser−Gly$_4$−Tyr tag
DPBS = Dulbecco's phosphate buffered saline solution *without* Ca^{2+} or Mg^{2+}

REFERENCES

(1) El Muslemany, K. M.; Twite, A. A.; ElSohly, A. M.; Obermeyer, A. C.; Mathies, R. A.; Francis, M. B. Photoactivated Bioconjugation Betweenortho-Azidophenols and Anilines: A Facile Approach to Biomolecular Photopatterning. *J. Am. Chem. Soc.* **2014**, *136*, 12600−12606.
(2) Furst, A. L.; Smith, M. J.; Francis, M. B. Direct Electrochemical Bioconjugation on Metal Surfaces. *J. Am. Chem. Soc.* **2017**, *139*, 12610−12616.
(3) Twite, A. A.; Hsiao, S. C.; Onoe, H.; Mathies, R. A.; Francis, M. B. Direct Attachment of Microbial Organisms to Material Surfaces Through Sequence-Specific DNA Hybridization. *Adv. Mater.* **2012**, *24*, 2380−2385.
(4) Gartner, Z. J.; Bertozzi, C. R. Programmed Assembly of 3-Dimensional Microtissues with Defined Cellular Connectivity. *Proc. National Acad. Sci.* **2009**, *106*, 4606−4610.
(5) Li, D.; Li, X.; Zhou, W.-L.; Huang, Y.; Liang, X.; Jiang, L.; Yang, X.; Sun, J.; Li, Z.; Han, W.-D.; Wang, W. Genetically Engineered T Cells for Cancer Immunotherapy. *Signal Transduct. Target Ther.* **2019**, *4*, 35.
(6) Abbina, S.; Siren, E. M. J.; Moon, H.; Kizhakkedathu, J. N. Surface Engineering for Cell-Based Therapies: Techniques for Manipulating Mammalian Cell Surfaces. *ACS Biomater. Sci. Eng.* **2018**, *4*, 3658−3677.
(7) Stephan, M. T.; Irvine, D. J. Enhancing Cell Therapies from the Outside in: Cell Surface Engineering Using Synthetic Nanomaterials. *Nano Today.* **2011**, *6*, 309−325.
(8) Shearer, R. F.; Saunders, D. N. Experimental Design for Stable Genetic Manipulation in Mammalian Cell Lines: Lentivirus and Alternatives. *Genes Cells.* **2015**, *20*, 1−10.
(9) Kohn, D. B.; Sadelain, M.; Glorioso, J. C. Occurrence of Leukaemia Following Gene Therapy of X-Linked SCID. *Nat. Rev. Cancer.* **2003**, *3*, 477−488.
(10) Prescher, J. A.; Dube, D. H.; Bertozzi, C. R. Chemical Remodelling of Cell Surfaces in Living Animals. *Nature.* **2004**, *430*, 873−877.
(11) Baskin, J. M.; Prescher, J. A.; Laughlin, S. T.; Agard, N. J.; Chang, P. V.; Miller, I. A.; Lo, A.; Codelli, J. A.; Bertozzi, C. R. Copper-Free Click Chemistry for Dynamic in Vivo Imaging. *Proc. National Acad. Sci.* **2007**, *104*, 16793−16797.
(12) Saxon, E.; Bertozzi, C. R. Cell Surface Engineering by a Modified Staudinger Reaction. *Science.* **2000**, *287*, 2007−2010.
(13) Wang, X.; Lang, S.; Tian, Y.; Zhang, J.; Yan, X.; Fang, Z.; Weng, J.; Lu, N.; Wu, X.; Li, T.; Cao, H.; Li, Z.; Huang, X. Glycoengineering of Natural Killer Cells with CD22 Ligands for Enhanced Anticancer Immunotherapy. *ACS Central Sci.* **2020**, *6*, 382−389.
(14) Frank, M. J.; Olsson, N.; Huang, A.; Tang, S.-W.; Negrin, R. S.; Elias, J. E.; Meyer, E. H. A Novel Antibody-Cell Conjugation Method to Enhance and Characterize Cytokine-Induced Killer Cells. *Cytotherapy.* **2020**, *22*, 135−143.
(15) Li, H.-K.; Hsiao, C.-W.; Yang, S.-H.; Yang, H.-P.; Wu, T.-S.; Lee, C.-Y.; Lin, Y.-L.; Pan, J.; Cheng, Z.-F.; Lai, Y.-D.; Hsiao, S.-C.; Tang, S.-W. A Novel Off-the-Shelf Trastuzumab-Armed NK Cell Therapy (ACE1702) Using Antibody-Cell-Conjugation Technology. *Cancers.* **2021**, *13* (11), 2724.
(16) Pishesha, N.; Bilate, A. M.; Wibowo, M. C.; Huang, N.-J.; Li, Z.; Deshycka, R.; Bousbaine, D.; Li, H.; Patterson, H. C.; Dougan, S. K.; Maruyama, T.; Lodish, H. F.; Ploegh, H. L. Engineered Erythrocytes Covalently Linked to Antigenic Peptides Can Protect against Autoimmune Disease. *Proc. National Acad. Sci.* **2017**, *114*, 3157−3162.
(17) Shi, J.; Kundrat, L.; Pishesha, N.; Bilate, A.; Theile, C.; Maruyama, T.; Dougan, S. K.; Ploegh, H. L.; Lodish, H. F. Engineered Red Blood Cells as Carriers for Systemic Delivery of a Wide Array of Functional Probes. *Proc. National Acad. Sci.* **2014**, *111*, 10131−10136.
(18) Harmand, T. J.; Pishesha, N.; Rehm, F. B. H.; Ma, W.; Pinney, W. B.; Xie, Y. J.; Ploegh, H. L. Asparaginyl Ligase-Catalyzed One-Step Cell Surface Modification of Red Blood Cells. *ACS Chem. Biol.* **2021**, *16*, 1201−1207.
(19) Li, J.; Chen, M.; Liu, Z.; Zhang, L.; Felding, B. H.; Moremen, K. W.; Lauvau, G.; Abadier, M.; Ley, K.; Wu, P. A Single-Step Chemoenzymatic Reaction for the Construction of Antibody−Cell Conjugates. *ACS Central Sci.* **2018**, *4*, 1633−1641.
(20) Maza, J. C.; Bader, D. L. V.; Xiao, L.; Marmelstein, A. M.; Brauer, D. D.; ElSohly, A. M.; Smith, M. J.; Krska, S. W.; Parish, C. A.; Francis, M. B. Enzymatic Modification of N-Terminal Proline Residues Using Phenol Derivatives. *J. Am. Chem. Soc.* **2019**, *141*, 3885−3892.
(21) Lobba, M. J.; Fellmann, C.; Marmelstein, A. M.; Maza, J. C.; Kissman, E. N.; Robinson, S. A.; Staahl, B. T.; Urnes, C.; Lew, R. J.; Mogilevsky, C. S.; Doudna, J. A.; Francis, M. B. Site-Specific Bioconjugation through Enzyme-Catalyzed Tyrosine−Cysteine Bond Formation. *ACS Central Sci.* **2020**, *6*, 1564−1571.
(22) Marmelstein, A. M.; Lobba, M. J.; Mogilevsky, C. S.; Maza, J. C.; Brauer, D. D.; Francis, M. B. Tyrosinase-Mediated Oxidative Coupling of Tyrosine Tags on Peptides and Proteins. *J. Am. Chem. Soc.* **2020**, *142*, 5078−5086.
(23) Bruins, J. J.; Westphal, A. H.; Albada, B.; Wagner, K.; Bartels, L.; Spits, H.; van Berkel, W. J. H.; van Delft, F. L. Inducible, Site-Specific Protein Labeling by Tyrosine Oxidation−Strain-Promoted (4 + 2) Cycloaddition. *Bioconjugate Chem.* **2017**, *28*, 1189−1193.
(24) Wilton, E. E.; Opyr, M. P.; Kailasam, S.; Kothe, R. F.; Wieden, H.-J. SdAb-DB: The Single Domain Antibody Database. *ACS Synth. Biol.* **2018**, *7*, 2480−2484.
(25) Kirchhofer, A.; Helma, J.; Schmidthals, K.; Frauer, C.; Cui, S.; Karcher, A.; Pellis, M.; Muyldermans, S.; Casas-Delucchi, C. S.; Cardoso, M. C.; Leonhardt, H.; Hopfner, K.-P.; Rothbauer, U. Modulation of Protein Properties in Living Cells Using Nanobodies. *Nat. Struct. Mol. Biol.* **2010**, *17*, 133−138.
(26) Morvan, M. G.; Lanier, L. L. NK Cells and Cancer: You Can Teach Innate Cells New Tricks. *Nat. Rev. Cancer.* **2016**, *16*, 7−19.
(27) Bald, T.; Krummel, M. F.; Smyth, M. J.; Barry, K. C. The NK Cell−Cancer Cycle: Advances and New Challenges in NK Cell−Based Immunotherapies. *Nat. Immunol.* **2020**, *21*, 835−847.
(28) Tam, Y. K.; Maki, G.; Miyagawa, B.; Hennemann, B.; Tonn, T.; Klingemann, H.-G. Characterization of Genetically Altered, Interleukin 2-Independent Natural Killer Cell Lines Suitable for Adoptive Cellular Immunotherapy. *Hum. Gene Ther.* **1999**, *10*, 1359−1373.
(29) Suck, G.; Odendahl, M.; Nowakowska, P.; Seidl, C.; Wels, W. S.; Klingemann, H. G.; Tonn, T. NK-92: An 'off-the-Shelf Therapeutic' for Adoptive Natural Killer Cell-Based Cancer Immunotherapy. *Cancer Immunol. Immunother.* **2016**, *65*, 485−492.
(30) Obermeyer, A. C.; Jarman, J. B.; Francis, M. B. N-Terminal Modification of Proteins with O-Aminophenols. *J. Am. Chem. Soc.* **2014**, *136*, 9572−9579.
(31) Hurben, A. K.; Erber, L. N.; Tretyakova, N. Y.; Doran, T. M. Proteome-Wide Profiling of Cellular Targets Modified by Dopamine Metabolites Using a Bio-Orthogonally Functionalized Catecholamine. *ACS Chem. Biol.* **2021**, *16*, 2581−2594.
(32) Bruce, V. J.; Lopez-Islas, M.; McNaughton, B. R. Resurfaced Cell-Penetrating Nanobodies: A Potentially General Scaffold for Intracellularly Targeted Protein Discovery. *Protein Sci.* **2016**, *25*, 1129−1137.
(33) Lyon, R. Drawing Lessons from the Clinical Development of Antibody-Drug Conjugates. *Drug Discovery Today Technologies.* **2018**, *30*, 105−109.

https://doi.org/10.1021/acscentsci.1c01265
ACS Cent. Sci. 2022, 8, 955−962

(34) Bauer, S.; Groh, V.; Wu, J.; Steinle, A.; Phillips, J. H.; Lanier, L. L.; Spies, T. Activation of NK Cells and T Cells by NKG2D, a Receptor for Stress-Inducible MICA. *Science.* **1999**, *285*, 727−729.

https://doi.org/10.1021/acscentsci.1c01265
ACS Cent. Sci. 2022, 8, 955−962